

Effect of RP-1 Compositional Variability on Thermal Conductivity at High Temperatures and High Pressures

L.A. Akhmedova-Azizova,[†] I.M. Abdulagatov,^{*,‡} and T.J. Bruno[‡]

[†]Azerbaijan State Oil Academy, Azadlig Ave., Baku, Az1010, 370601, Azerbaijan, and [‡]Thermophysical Properties Division, National Institute of Standards and Technology, 325 Broadway, Boulder, Colorado 80305-3337, USA

Received May 11, 2009. Revised Manuscript Received June 29, 2009

The thermal conductivity of rocket propellant RP-1 has been measured with a coaxial-cylinder (steady-state) technique. Measurements were made in the temperature range from 292 to 732 K and at pressures up to 60 MPa. The expanded uncertainties of thermal conductivity, pressure, and temperature measurements at the 95% confidence level with a coverage factor of $k = 2$ were estimated to be 2%, 0.05%, and 30 mK, respectively. The thermal conductivity data for RP-1 reported in this work do not include the correction to radiation. Therefore, the uncertainty of the data is larger than 2%. The onset of the effects of thermal decomposition (chemical reaction) on the thermal conductivity of RP-1 at temperatures was found above approximately 650 K. The measured values of thermal conductivity were compared with the data reported in the literature and with the values calculated from a correlation equation. The average absolute deviation (AAD) between the present data and the values reported in the literature was 1.0%. An empirical model was developed to predict the thermal conductivity of RP-1 (within 2.0%) with just the thermal conductivity values as a function of pressure at reference temperature $T_0 = 293$ K, $\lambda_0(P)$, as input.

Introduction

Reliable transport and thermodynamic properties of rocket propellant RP-1 fuel are needed in many applications, such as calculation of optimal design parameters, efficient operation of high-temperature rocket engines, analysis of the design and performance of a rocket propulsion system for rational design of highly reliable rocket engine systems, prediction of heat- and mass-transfer coefficients in both laminar and turbulent regimes, and in the development of equations of state to represent fluid properties. The thermal conductivity plays a key role in these activities and processes. A literature survey reveals that only one experimental data set, reported by Magee et al.,¹ is available for the thermal conductivity of the RP-1. Those measurements were performed with the transient hot wire technique in the temperature range from 300 to 700 K and at pressures up to 70 MPa. These workers found rapid serious decomposition of the RP-1 sample at temperatures beginning at approximately 650–700 K. The uncertainty in the thermal conductivity measurements¹ at temperatures from 300 to 450 K is less than 0.5%, whereas at higher temperatures (approximately 550 K), where decomposition and the effect of radiation is significant, the uncertainty is approximately 1.0%. At temperatures starting at 650 K, the uncertainty is about 4% due to large changes in sample composition. It was noted in ref 1 that the sample used for these measurements was unusual, in that it comprised an unusually high olefin and aromatic content.

The composition-explicit distillation curve of RP-1 (an approximation of the vapor–liquid equilibrium of this com-

plex fluid) was measured by Bruno and Smith.² Magee et al.¹ reported a comprehensive review of available experimental thermal conductivity and other thermophysical properties data for RP-1 and related constituent compounds.

The main objective of this work is to illustrate how compositional variability in the initial sample and in the fluid after thermal stress can affect measured thermal conductivity. The fluid measured in this work is the same as that used by Magee et al.,¹ and measurements were made from 292 to 732 K and pressures to 60 MPa.

Experimental Section

RP-1 Samples. Two samples (A and B) of RP-1 were supplied by the Fuels Branch of the Air Force Research Laboratory (AFRL, Wright Patterson Air Force Base). The samples were drawn directly from the supply containers with disposable pipettes. The fluid was not permitted to come into contact with the can exterior. Approximately 0.5 mL of the fluid was drawn and stored in a tightly capped scintillation vial at room temperature until used. The duration of this storage period was less than 1 h before the analysis was completed. Both samples had a pale red cast provided by a dyeing agent, azobenzene-4-azo-2-naphthol, and both appeared to have the viscosity and odor of typical kerosene.

The samples were analyzed with a gas chromatography – mass spectrometry – infrared spectrophotometry method.^{3,4} A 30 m capillary column with a 0.1 μm coating of 5% phenyl polydimethyl siloxane was chosen as the stationary phase. This phase provides separations based upon boiling temperature and

*To whom correspondence should be addressed. E-mail: ilmutdin@boulder.nist.gov.

(1) Magee, J. W.; Bruno, T. J.; Friend, D. G.; Huber, M. L.; Laesecke, A.; Lemmon, E. W.; McLinden, M. O.; Perkins, R. A.; Baranski, J.; Widegren, J. A. Thermophysical properties measurements and models for rocket propellant RP-1: Phase I. *NISTIR 6646*; 2007.

(2) Bruno, T. J.; Smith, B. L. *Ind. Eng. Chem. Res.* **2006**, *45*, 4381–4388.

(3) Bruno, T. J.; Svoronos, P. D. N. *CRC Handbook of Basic Tables for Chemical Analysis*, 2nd ed.; Taylor and Francis CRC Press: Boca Raton, 2004.

(4) Bruno, T. J.; Svoronos, P. D. N. *CRC Handbook of Fundamental Spectroscopic Correlation Charts*; Taylor and Francis CRC Press: Boca Raton, 2005.

Table 1. Thermal Decomposition Reaction Rate Constants for Two Samples of RP-1

temperature, K	RP-1, sample A ($k \pm 1\sigma$), s ⁻¹	RP-1, sample B ($k \pm 1\sigma$), s ⁻¹
648.15	$(6.92 \pm 0.75) \times 10^{-5}$	$(1.13 \pm 0.04) \times 10^{-5}$
673.15	$(2.00 \pm 0.23) \times 10^{-4}$	$(1.19 \pm 0.33) \times 10^{-4}$
698.15	$(3.85 \pm 0.53) \times 10^{-4}$	$(3.08 \pm 0.77) \times 10^{-4}$
723.15		$(5.84 \pm 1.33) \times 10^{-4}$
773.15	$(1.07 \pm 0.17) \times 10^{-3}$	

also the polarity of the solute. In this context, polarity also includes points of unsaturation or aromaticity on the solute molecule. Sample was injected via syringe into a split/splitless injector set with a 100 to 1 split ratio. The injector was operated at a temperature of 623 K and a constant head pressure of 0.1565 MPa. The sample residence time in the injector was very short, thus the effect of sample exposure to this high temperature is expected to be minimal. The column was temperature programmed to provide complete and rapid elution with minimal loss of peak shape. Initially, the temperature was maintained isothermally at 333 K for 2 min, followed by a 275 K/min ramp to 363 K, followed by a 283 K/min ramp to 523 K. Although the analysis was allowed to run for 40 min, all peaks were eluted after approximately 27 min. Mass spectra were collected for each peak from 15 to 550 RMM (relative molecular mass) units, and infrared spectra were collected from between 4000 and 600 cm⁻¹. Integration of the areas under each peak was done with a commercial algorithm optimized to identify peaks that were at least an order of magnitude larger than the noise level. Overall, both samples of RP-1 showed approximately 350 peaks that could be easily distinguished from noise level, and perhaps twice that number that were barely above noise level. In addition to analysis by GC-MS-IR, a total sulfur analysis was done by GC with a sulfur chemiluminescence detector (SCD), and a copper strip corrosion test was done. The results of the SCD and copper strip test indicated that both samples were very low in sulfur (less than 30 ppm mass/mass).

As mentioned earlier, the first sample (A) was unusual in that chemical analysis showed a much larger fraction of olefinic and aromatic compounds than would be expected in a typical kerosene fraction. Approximately 20% of the compounds identified in this mixture had a double bond or an aromatic ring. It is therefore not representative of an on-specification RP-1. The second sample (B) was more typical of a kerosene rocket propellant, with very low olefinic and aromatic fractions. The detailed analytical results for both fluids are available elsewhere.^{1,2,5,6} Because of the unusual composition profile, the analyses are presented in four parts: components in excess of 1% of the total (mass/mass), light components, heavy components, and trace components. The reader should consult the references for details. Sample B is considered to be representative of typical as-delivered RP-1, a fluid that has a relatively tighter specification than commodity fuels such as aviation fuel, diesel fuel, or gasoline.⁷

Chemical analysis studies were also done on the samples of RP-1 after exposure to elevated temperatures. These studies were done in two separate protocols. The first was a kinetic thermal decomposition study performed before property measurements were made, in an effort to determine the regions in which thermal decomposition would adversely affect property measurements. This work provided pseudofirst-order rate constants and half-lives for both samples of RP-1. The second protocol that was applied consisted of chemical analysis after

exposure to high temperatures while property measurements were performed. We will describe both protocols separately below.

Thermal Decomposition Kinetics of RP-1. The thermal decomposition kinetics of both RP-1 samples were determined using a method that we previously developed specifically for complex fluids.^{8–13} We have applied this technique to a variety of fluids in addition to rocket propellants, including aviation fuels, missile fuels, and organic Rankine cycle fluids. With this method, the fuel is decomposed in ampule reactors made of 316 L stainless steel, and the extent of decomposition is determined as a function of time by gas chromatography. The resulting data are used to derive global pseudofirst-order rate constants that approximate the overall decomposition rate of the mixture. Since the rate measurements are done at different temperatures, they can be used to estimate Arrhenius parameters for the prediction of rate constants at other temperatures. These studies typically require a separate chemical analysis of the decomposed vapor and liquid phases of the fuels, a task performed with a specially constructed flow conditioner.¹⁴ In Table 1, we present the thermal decomposition reaction rate constants measured for both samples of RP-1.^{8,12} The effect of the higher concentration of olefinic compounds found in sample A is evident from the relatively higher reaction rates.

The results in Table 1 are significant in that they allow one to rationally plan for decomposition and design residence times in the measurement of thermophysical properties. In general, the fluids are relatively stable vis a vis thermophysical property measurement up to approximately 673 K. Above this temperature, more careful consideration must be given to residence time. At temperatures near 773 K, the decomposition is rapid and residence times must be less than two or three minutes in a typical thermophysical property instrument.

Chemical Analysis of Thermally Stressed Fuel. The second protocol consisted of recovery of thermally stressed samples of RP-1 from the thermal conductivity measurement apparatus, after operation at high temperatures. This is not unrelated to the first protocol, especially at the higher temperatures, since very similar chemistries were observed to occur. It is impossible to provide a uniform description of the behavior of all of the thermally stressed samples, because of the variation in temperatures and pressures, and of wetted surfaces. One can, however, provide some general characteristics that typically result from exposure of RP-1 to these conditions. Samples that have been stressed above 723 K for even a short time usually appear brown because of the development of carbonaceous solids in suspension. The viscosity is typically higher than the unstressed fluid

(8) Andersen, P. C.; Bruno, T. J. *Ind. Eng. Chem. Res.* **2005**, *44* (6), 1670–1676.

(9) Andersen, W. A.; Bruno, T. J. *Ind. Eng. Chem. Res.* **2005**, *44*, 5560–5566.

(10) Widegren, J. A.; Bruno, T. J. *Ind. Eng. Chem. Res.* **2008**, *47* (13), 4342–4348.

(11) Widegren, J. A.; Bruno, T. J. *Ind. Eng. Chem. Res.* **2008**, submitted.

(12) Widegren, J. A.; Bruno, T. J. *Ind. Eng. Chem. Res.* **2008**, submitted.

(13) Bruno, T. J.; Huber, M. L.; Laesecke, A.; Lemmon, E. W.; Perkins, R. A. *Thermochemical and Thermophysical Properties of JP-10, NIST-IR 6640*; National Institute of Standards and Technology: U.S., 2006.

(14) Bruno, T. J. *Sep. Sci. Technol.* **2005**, *40* (8), 1720–1732.

(5) Bruno, T. J.; Andersen, P. C.; Widegren, J. *RP-1 sample compositional variability, Wright Laboratory Aero Propulsion and Power Directorate, Final Report, MIPR NGWSPR00472412*; Wright Patterson Air Force Base: 2005.

(6) Widegren, J. A.; Bruno, T. J. *The Properties of RP-1 and RP-2, Interim Report, MIPR F15BAA8022G001*; March, 2008.

(7) Purchase Description, RP-1, MIL-DTL-25576E Federal Business Opportunities, <http://fs2.eps.gov/EPSPData/DLA/Synopses/12671/SP0600-03-R-0322/rp-1sol.pdf>. Accessed: April 14, 2006.

Table 2. Results of ASTM-2789 on RP-1 Sample A, Used for Thermal Conductivity Measurements at 784.15 K

fraction	RP-1, sample A, unstressed	RP-1, sample A, after exposure to 784.15 K
paraffins	40.3	4.0
monocycloparaffins	32.8	12.6
dicycloparaffins	19.4	9.0
aromatics, (1 ring)	5.7	41.5
indanes and tetralins	0.8	12.7
naphthalenes	1.0	20.2

as well. The mass spectral total ion chromatogram of the stressed fluid is usually remarkable in that the typical Gaussian-like distribution of constituents encountered in a kerosene is absent. Rather, there are a number of large, early eluting peaks, followed by a relatively uniform distribution of peaks for the remainder of the chromatogram. Also remarkable is the complete disappearance of some major constituents of RP-1 after thermal stress. Thus, *n*-dodecane, a major constituent of unstressed RP-1, is typically absent from samples stressed to 773 K. The time required for this to occur has not been fully investigated.

A useful method in characterizing the overall composition, and comparing stressed and unstressed samples, is an adaptation of ASTM Method 2789.^{15,16} In this method, one uses mass spectrometry (or gas chromatography – mass spectrometry) to characterize hydrocarbon samples into six types. The six types or families are paraffins, monocycloparaffins, dicycloparaffins, alkylbenzenes (arenes or aromatics), indanes and tetralins (grouped as one classification), and naphthalenes. Although the method is specified only for application to low olefinic gasolines, and it has significant limitations, it is of practical relevance to many complex fluid analyses and is often applied to gas turbine fuels, diesel fuels, rocket propellants, and missile fuels. The uncertainty of this method, and the potential pitfalls, were treated elsewhere.^{2,16} As an example of how this method provides a comparison of thermally stressed and unstressed fuels, we present in Table 2 results for unstressed RP-1, sample A, and a sample withdrawn from the thermal conductivity apparatus used in this work after measurement that terminated at 732 K. The data are provided as volume fractions. This table shows in dramatic fashion the effects of thermal stress and is consistent with the observations made earlier from the decomposition kinetics protocol. We note the decrease of paraffins and the increase of aromatics, as expected. Also very striking is the emergence of significant naphthalenic compounds. The appearance of these compounds is actually the reason why it is useful to include infrared spectrophotometric detection to the chromatographic analysis discussed earlier.

Thermal Conductivity Apparatus. The thermal conductivity of the RP-1 sample was measured by a coaxial-cylinder (steady-state) technique. The method (apparatus, procedure of measurements,

calibration procedure, and uncertainty assessment) has been described fully in previous publications,^{17–23} thus only a brief review will be given here. With this method, the heat generated in an inner emitting cylinder is conducted radially through the narrow, fluid-filled annulus to a coaxial receiving cylinder. The heart of the apparatus consisted of a high-pressure autoclave, thermostat, and the thermal conductivity cell. The autoclave was made from stainless steel 1X18H10T and was located in the thermostat. The thermostat was a massive, solid copper block. The thermal conductivity cell consisted of two coaxial cylinders: an inner (emitting) cylinder with diameter d_2 of 10.98×10^{-3} m (repeatability $\pm 0.1 \times 10^{-4}$ m) and an outer (receiving) cylinder with diameter d_1 of 12.92×10^{-3} m (repeatability $\pm 0.2 \times 10^{-4}$ m). The length of the measuring section of the inner cylinder (emitter) was $l = 150 \times 10^{-3}$ m (repeatability $\pm 1 \times 10^{-4}$ m). The gap between cylinders (thickness of the liquid gap) was $d = 0.97 \times 10^{-3}$ m (repeatability $\pm 0.03 \times 10^{-3}$ m). Theoretically, it is assumed that a thin layer of a homogeneous fluid is enclosed between two coaxial cylinders of infinite length, in which case, the end effect is zero. In practice, the length of the cylinders is not infinite and the heat transfer through the ends must be considered. The theory of this type of thermal conductivity cell has been discovered in ref 24. The acceptable value (see ref 25) for the thickness of the liquid layer d is between 0.5 and 1.0 mm. If $d > 1.0$ mm, the development of natural convection heat transfer is possible.^{24,25} The optimal ratio of the length l to the diameter of the inner cylinder d_2 should be $l/d_2 = 10–15$ (see refs 24 and 25). It is very difficult to maintain the homogeneity of the temperature distribution along the length of inner cylinder when the ratio $l/d_2 > 15$. If $l/d_2 < 10$, the end effects are typically significant.^{24,25}

The centering of the outer and inner cylinders was achieved by a micro screw adjustment. The deviation from concentricity was 0.002 cm, or 2% of the sample layer. This is important, because the deviation of the cylinders from concentricity (skew of the inner and outer cylinder axes) can cause convection. The inner cylinder was mounted coaxially in the outer cylinder by using the centering mechanism. The centering mechanism is made of textolite and attached to micro screws that are located in the two sections of the outer cylinders. The micro screws are used to adjust the vertical position of the cylinders. To minimize the deviation of the inner and outer cylinders from the eccentricity, the cylindrical bushes also were used. The thickness of the walls of bushes are exactly the same as a size of the measuring liquid gap. The centering of the outer and inner cylinders was checked with a cathetometer (CM-8). At low temperatures (below 573 K), in order to center the cylinders, the centering rings also were used.

The temperature, T , in the thermostat was controlled with a three-section heating element. A platinum resistance thermometer and three chromel–alumel thermocouples were located on the copper block. The temperature differences between various sections (or levels) of the copper block were within 0.02 K. The pressure, P , in the system was generated and measured with piston manometers that had upper limits of 60 and 600 bar. In the cell, heat was generated by a microheater that consists of an isolated (high temperature, lacquer covered) constantan wire of 0.1 mm diameter wound on a ceramic tube

(15) Standard test method for hydrocarbon types in low olefinic gasoline by mass spectrometry, *ASTM Standard D 2789–04b, Book of Standards*; American Society for Testing and Materials: West Conshohocken, PA, 2005; Vol 05.01.

(16) Smith, B. L.; Bruno, T. J. *Ind. Eng. Chem. Res.* **2007**, *46*, 310–320.

(17) Abdulagatov, I. M.; Assael, M. J. Thermal conductivity. In *Hydrothermal Properties of Materials. Experimental Data on Aqueous Phase Equilibria and Solution Properties at Elevated Temperatures and Pressures*. Valyashko, V.M., Ed.; John Wiley & Sons: London, 2009. Ch 5, pp 227–249.

(18) Akhundov, T. C.; Iskenderov, A. I.; Akhmedova, L. A. *Izv. Vuzov, ser. Neft i Gas* **1995**, *1*, 56–58.

(19) Abdulagatov, I. M.; Akhmedova-Azizova, L. A.; Azizov, N. D. *J. Chem. Eng. Data* **2004**, *49*, 1727–1737.

(20) Abdulagatov, I. M.; Akhmedova-Azizova, L. A.; Azizov, N. D. *J. Chem. Eng. Data* **2004**, *49*, 688–704.

(21) Akhmedova-Azizova, L. A. *J. Chem. Eng. Data* **2006**, *51*, 2088–2090.

(22) Akhmedova-Azizova, L. A.; Babaeva, S.Sh. *J. Chem. Eng. Data* **2008**, *53*, 462–465.

(23) Akhmedova-Azizova, L. A.; Abdulagatov, I. M. *J. Sol. Chem.* **2008**, in press.

(24) Gershuni, G. Z. *Dok. Akad. Nauk USSR* **1952**, *86*, 697–698.

(25) Rastorguev, Yu.L.; Nemzer, B. G. *Teploenergetika* **1968**, *12*, 78–82.

(of a 2 mm diameter) with the same length as the inner cylinder. The microheater was located inside the inner cylinder (closely fitted inside the emitter). The wire was uniformly wound on the ceramic tube with a pitch of 0.35 mm. This was meant to provide heat flux uniformly, generated in the inner cylinder and propagated radially through the fluid under study to the outer cylinder in a steady state condition.

The thermal conductivity, λ , of the fluid was deduced from measurements of heat, Q , transmitted across the fluid layer; the temperature difference, ΔT , between the inner and outer cylinders; the thickness of the fluid layer, d ; and the effective length, l , of the measuring part of the cylinder as:

$$\lambda = A \frac{Q_{\text{meas}} - Q_{\text{los}}}{\Delta T_{\text{meas}} - \Delta T_{\text{corr}}} \quad (1)$$

where $A = [\ln(d_2/d_1)]/2\pi l$ is a geometric parameter (cell constant) of the thermal conductivity cell (which can be determined from the geometrical characteristics of the experimental cell or by calibration^{17–19}); Q_{meas} is the amount of heat released by the calorimetric microheater; Q_{los} is the amount of heat losses through the ends of the measuring cell (end effect); $\Delta T_{\text{corr}} = \Delta T_{\text{cl}} + \Delta T_{\text{lac}}$; ΔT_{cl} and ΔT_{lac} are the temperature differences in the cylinder walls and lacquer coat, respectively; and ΔT_{meas} is the temperature difference measured with differential thermocouples.

The values of Q_{meas} and ΔT_{meas} are measured indirectly, thus some corrections are necessary. The corrections Q_{los} and ΔT_{corr} were estimated by measuring a standard liquid (toluene) with its well-known thermal conductivity.^{26,27} This calibration was made at several selected temperatures between 290 and 700 K, and at 5 selected pressures between 0.1 and 30 MPa. In these temperature and pressure ranges, the estimated value of Q_{los} varies within 0.3–0.05 W. This value is negligibly small (0.38%) in comparison to the heat transfer by conduction, $Q = 13.06$ W.

As is well-known, convective heat transfer increases with increasing values of the Rayleigh number (Ra). To reduce the values of Ra, a small gap distance between cylinders, $d = 0.97 \times 10^{-3}$ m, was used. In the range of the present experiments, the values of Ra were always less than 500 (the critical value is $Ra_c = 1000$ for this method²⁴), and convective heat transfer, Q_{con} , was estimated to be negligibly small. The absence of convection can be verified experimentally by measuring the thermal conductivity with various temperature differences ΔT (1–3 K) across the fluid gap, and with different heating powers, Q , transferred from the inner to the outer cylinder. The measured thermal conductivities were indeed independent of the applied temperature differences ΔT and power Q .

Any conductive heat transfer is accompanied by simultaneous radiative transfer. The correction for thermal radiation depends upon whether or not the fluid absorbs radiation. To minimize the radiation emission of the cylinders, the inner and outer cylinder surfaces were highly polished and protected against oxidation. The emissivities, ϵ_1 and ϵ_2 , of the cylinders surfaces were small, and heat flux arising from radiation:

$$Q_{\text{rad}} = \sigma \left[\frac{1}{\epsilon_1} + \frac{S_1}{S_2} \left(\frac{1}{\epsilon_2} - 1 \right) \right] (T_1^4 - T_2^4) \quad (2)$$

was negligible (approximately 0.03 W) in comparison to the heat transfer ($Q = 13.06$ W) by conduction in the temperature range of our experiment. In eq 2, T_1 and T_2 are the temperatures of the cylinder surfaces; ϵ_1 and ϵ_2 are the emissivities of the cylinder surfaces at temperatures T_1 and T_2 , respectively; and S_1 and S_2 are the internal and external surface areas of the fluid layer,

respectively. To minimize the heat transfer by radiation, a solid material (stainless-steel 1X18H9T) of low emissivity was used for the cylinders, and thin layers of fluid were used. Radiation originated from the RP-1 sample, which can be a multiple of the radiation emitted from the cylinders. If the fluid is entirely transparent, the conductive and radiative heat fluxes are additive and independent. In this case, the correction is simple and usually negligible. When the fluid absorbs and re-emits radiation (partially transparent), the problem is more complicated since the radiative and conductive fluxes are coupled. In this case, the effect of heat transferred by radiation can be derived from the solution of the nonlinear integral–differential equation describing coupled radiation and conduction. Unfortunately, the explicit solution of this equation is impossible, and only a numerical solution is possible even after simplification, due to lack of the characteristic optical properties (refractive index and absorption coefficient) of RP-1 at high temperatures. Therefore, the present thermal conductivity data for RP-1 do not include the correction to radiation. The data reported by Magee et al.¹ also do not include such a radiation correction.

Measurement uncertainties exist in the measured quantities contained in working eq 1 (A , Q , ΔT) and the uncertainties of the temperature, T , and pressure, P , measurements. The uncertainty in all of the measured quantities was $S_A = 0.0009 \text{ m}^{-1}$, $S_Q = 2.6 \cdot 10^{-3} \text{ W}$, $S_{\Delta T} = 0.005 \text{ K}$, $S_T = 0.03 \text{ K}$, and $S_P = 0.03 \text{ MPa}$. The value of the root-mean-square deviation of heat losses through the ends of the measuring cell is approximately $S_{Q_{\text{los}}} = 0.001 \text{ W}$. The uncertainties of the measured values d_1 , d_2 , and l are 0.15, 0.09, and 0.07%, respectively; the corresponding uncertainty of A is 0.5%. The uncertainty in measured heat flow, Q , is approximately 0.1%. To ensure the cell was in equilibrium, measurements were started 10 h after the time when the thermostat reached the prescribed temperature. From the uncertainty of the measured quantities and the corrections mentioned above, the total maximum relative uncertainty, $\delta\lambda/\lambda$, in measuring the thermal conductivity at temperatures below 600 K was 2%, whereas at high temperature (above 650 K) where decomposition of the sample is possible, the uncertainty is about 4–5%.

Results and Discussion

Measurements of the thermal conductivity for the RP-1 (sample A) were performed at eight isobars (0.1, 6, 10, 20, 30, 40, 50, and 60 MPa) in the temperature range between 292 and 732 K. Thermal conductivity measurements were made at constant pressure as a function of temperature. The possibility of the chemical reactions occurring during thermophysical property measurements at high temperatures has already been discussed. Since the RP-1 fuel sample is hydrocarbon-based, chemical decomposition of the sample is possible at temperatures above 650 K. Therefore, in thermal conductivity experiments when the RP-1 sample is confined in the measuring cell at temperatures above 650 K for several hours, the decomposition of the RP-1 sample may cause a significant effect on measured values of thermal conductivity. The magnitude of the decomposition effect depends on temperature, pressure, and residence time in the measuring cell.

After charging the measuring cell with fresh RP-1 sample, the measurements were started at low temperatures (about 293 K) with increasing temperatures along the isobar. To check the reproducibility of the thermal conductivity measurements and the effect of possible chemical decomposition of the RP-1 sample, the measurements for the selected isobars (0.1, 6, 10, and 20 MPa) were made in three runs. After the sample reached 600 K (Run-1, before the temperature where we expected possible decomposition), the sample was cooled to the initial temperature of 293 K, and the second run (Run-2) of

(26) Mamedov, A. M.; Akhundov, T. S. *Thermodynamic Properties of Gases and Liquids. Aromatic Hydrocarbons*; Moscow, Gosudarstvennaya Sluzhba Standartnyx Spravochnyx Dannyx, 1978; Vol 5.

(27) Ramires, M. L. V.; Nieto de Castro, C. A.; Perkins, R. A.; Nagasaka, Y.; Nagashima, A.; Assael, M. J.; Wakeham, W. A. *J. Phys. Chem. Ref. Data* **2000**, *29*, 133–139.

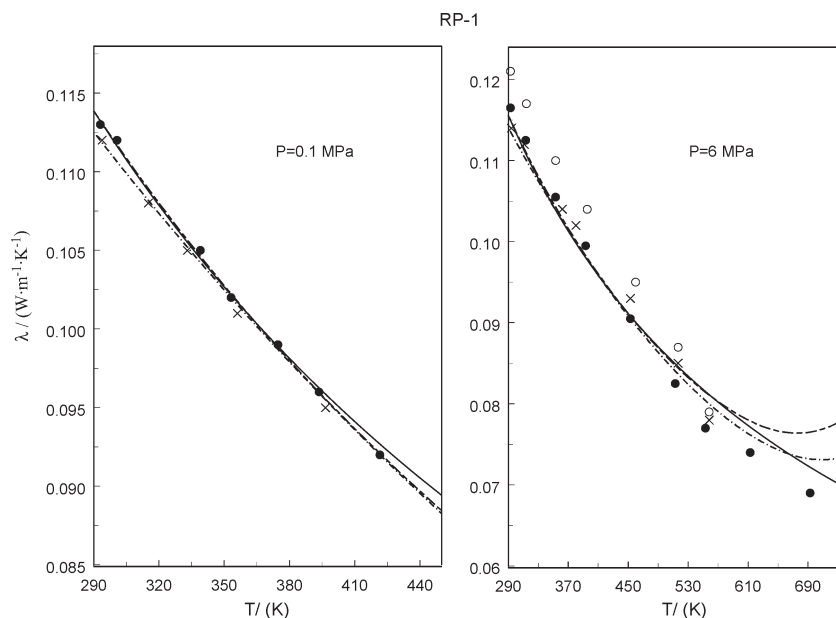


Figure 1. Measured and calculated values of the thermal conductivity of RP-1 (sample A) as a function of temperature at two selected isobars (0.1 and 6 MPa). (●), this work (Run-1); (×), this work (Run-2); (○), this work (Run-3); (—) surrogate model¹ (RP-1, sample A); (— · — · — · —), surrogate model²⁸ (RP-1, sample B); (— — —), this work (eq 3).

measurements was started with the same sample (previously heated to 600 K) by increasing the temperature. If decomposition has already occurred, a discrepancy between the first and second runs should be expected due to chemical composition changes in the sample. Differences between the first and second runs measurements were within their experimental uncertainties (2–2.5%). At temperatures below 600 K, we never observed significant differences between the thermal conductivities of the first (fresh) and second runs. No hysteresis in thermal conductivity behavior was found (see Figure 1). After long residence times (5–6 h) at temperatures below 600 K, we discharged the sample. No changes of the sample (except for the disappearance of the pink cast caused by the decomposition of the dye) and in the measuring cell were found. This procedure was repeated for the various isobars at temperatures below 600 K. If the sample was heated to temperatures above 630 K, then cooled to low temperature (293 K) and repeated again, the measurements (Run-3) showed significant differences (up to 5–10% and more) between both runs (Run-1 and 3) (see Figure 1). This clearly confirmed the effect of chemical decomposition (chemical composition changes) of the sample on the measured values of thermal conductivity. After completion of the measurements (Run-3) at high temperatures (around 730 K), the measuring cell was discharged and a black-colored solid material (deposit of the carbonaceous materials) coating the cylinder walls was found. After completion of the measurement for a given isobar (after Run-3), the measuring cell was discharged and new fresh sample was used to continue the measurements for the next isobar. This is a good way to test the effect of previous “thermal history” of the sample (preheating above decomposition temperature) on the measured values of thermal conductivity.

Just after reaching the desired temperature, the sample pressure was recorded as a function of time. Starting with the temperature above 650 K, we found that the pressure significantly changed with time. The rate of pressure changes varied in the range of 0.1 to 0.2 MPa per hour at a temperature of 650 K, depending on pressure. This is an indirect indication

of the chemical reaction in the sample at temperatures above 650 K.

The measured temperatures, pressures, and thermal conductivities are presented in Table 3. Some selected experimental results are shown in Figures 1 and 2 as λ - T and λ - P projections together with the values calculated from the correlation by Magee et al.¹ As Figure 1 shows, at constant pressures the thermal conductivity of the RP-1 decreases monotonically with increasing temperature. The pressure dependence of the thermal conductivity exhibits a small deviation from linearity.

A surrogate mixture model containing 14 constituent fluids to approximate the thermal conductivity behavior of the RP-1 (sample A) was reported in ref 1. The RP-1 is a complex hydrocarbon mixture; therefore, the properties depend on composition. Huber et al.²⁸ later developed correlation models for the two RP-1 samples with different compositions (samples A and B). The uncertainty of the calculated values of thermal conductivity is about 3%. The upper limit of validity of the correlation is about 600 K. The present results for thermal conductivity of RP-1 (sample A) and the data reported by Magee et al.¹ were compared with the values calculated from the correlation equation.¹ No systematic deviations were found for all of the measured data. The deviation statistics in the range from 292 to 630 K is Max. dev = 3.8%, AAD = 1.0%, Bias = -0.2%, Std. dev = 1.3%, and Std. err = 0.1%. As one can see, the agreement between the calculated and the measured values of thermal conductivity of the RP-1 in the range from 292 to 630 K is good (within 1.0%, less than the combined experimental uncertainty). At temperatures above 630 K, the deviations are large, 5–10% and more, due to decomposition. The direct comparison of our results with the data reported by Magee et al.¹ is somewhat inconvenient because of temperature and pressure differences between the measurements. The deviation plot between the correlation of ref 1 and both data sets is presented in Figure 3. As this figure shows, the agreement between the measured data sets is good (within 1–2%).

Table 3. Experimental Thermal Conductivities of RP-1 (λ , $\text{W} \cdot \text{m}^{-1} \cdot \text{K}^{-1}$)

pressure, MPa							
0.1 MPa		6 MPa		10 MPa		20 MPa	
<i>T</i>	λ	<i>T</i>	λ	<i>T</i>	λ	<i>T</i>	λ
293.15	0.113	293.18	0.116	293.15	0.114	293.15	0.120
293.95	0.112	294.20	0.114	300.65	0.115	299.65	0.116
300.75	0.112	311.40	0.112	317.15	0.110	300.72	0.118
315.15	0.108	313.42	0.113	333.19	0.107	325.85	0.112
333.15	0.105	338.19	0.109	339.17	0.108	345.15	0.109
339.14	0.105	353.21	0.106	353.20	0.106	353.21	0.111
353.24	0.101	362.27	0.104	353.17	0.106	353.25	0.109
356.14	0.101	374.75	0.106	359.15	0.103	365.15	0.107
374.75	0.099	380.32	0.102	374.67	0.102	374.75	0.106
393.65	0.096	393.31	0.099	393.68	0.100	393.61	0.104
396.65	0.095	453.05	0.091	421.85	0.096	421.60	0.100
421.65	0.092	453.13	0.093	453.05	0.093	475.79	0.095
453.15	0.084	512.89	0.083	475.83	0.090	533.11	0.091
		516.84	0.084	500.89	0.089	591.22	0.088
		553.21	0.077	533.05	0.085	614.03	0.082
		558.18	0.078	553.18	0.081	691.98*	0.078
		613.19	0.074	591.26	0.081	732.91*	0.074
		693.11*	0.069	613.23	0.076		
				693.08*	0.072		
				732.68*	0.068		
30 MPa		40 MPa		50 MPa		60 MPa	
<i>T</i>	λ	<i>T</i>	λ	<i>T</i>	λ	<i>T</i>	λ
293.01	0.123	292.98	0.127	292.00	0.129	293.05	0.131
313.51	0.119	313.04	0.123	313.38	0.125	313.02	0.127
353.03	0.113	352.87	0.116	353.11	0.117	353.98	0.119
393.41	0.107	392.84	0.111	393.14	0.112	393.02	0.116
453.55	0.101	453.46	0.105	453.05	0.107	453.85	0.109
512.52	0.095	523.67	0.098	514.09	0.101	527.89	0.103
554.98	0.092	550.73	0.097	554.18	0.099	598.18	0.099
617.23	0.089	613.23	0.094	613.23	0.095	673.23*	0.096
696.08*	0.085	693.38*	0.090	699.08*	0.093	735.08*	0.093
732.98*	0.084	732.76*	0.088	732.88*	0.092		

*The uncertainty is 4–10% and more; italic is Run-2.

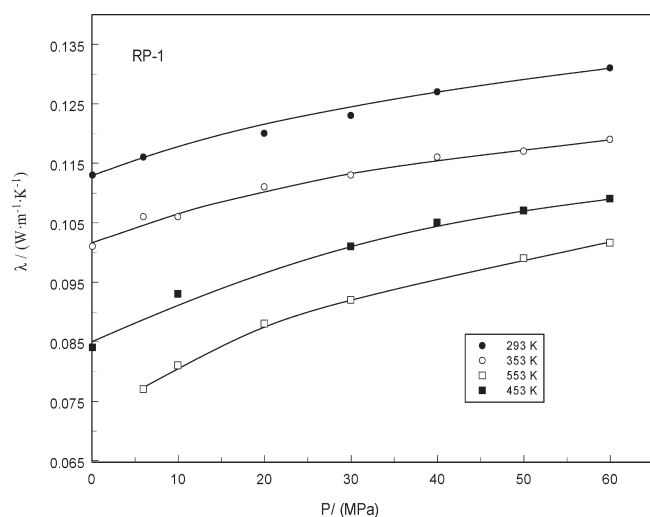


Figure 2. Measured values of thermal conductivity of RP-1 (sample A) as a function of pressure at five selected isotherms (some values were analytically interpolated).

Therefore, the agreement between the previous measurements reported by Magee et al.¹ and the present data is within their mutual uncertainty (see Figure 3).

(28) Huber, M.L.; Lemmon, E.W.; Ott, L. S.; Bruno, T.J. *Energy Fuels*, 2009, in preparation.

Figure 1 illustrate the good consistency of the temperature and pressure dependences of the thermal conductivity of RP-1 (sample A) measured in the present work and the values calculated with a correlation model.¹ In these figures, we also present the values of thermal conductivity calculated with Huber's model²⁸ for the second RP-1 sample (sample B), which has a more typical composition. As one can see from Figure 1, the thermal conductivity of the second RP-1 sample (B) calculated with the correlation model is systematically lower (by about 2–4% along the isobar at 10 MPa) than for the first RP-1 sample (A). This very clearly demonstrates how the sample composition affects the thermal conductivity.

Viswanath and Rao²⁹ proposed a predictive model for the thermal conductivity of liquids as

$$\left(\frac{\lambda(P, T)}{\lambda_0(P, T_0)} \right) = \left(\frac{T}{T_0} \right)^{-n} \quad (3)$$

where $\lambda_0(P, T_0)$ is the value of the thermal conductivity at T_0 , n is the empirical parameter. This equation can be used to predict the thermal conductivity of pure liquids and liquid mixtures at any temperature from a knowledge of the thermal conductivity values as a function of pressure at a reference temperature T_0 , $\lambda_0(P, T_0)$. Viswanath and Rao²⁹ and Klaas and Viswanath³⁰

(29) Viswanath, D. S.; Rao, M. B. *J. Phys. D: Appl. Phys.* 1970, 3, 1444–1450.

(30) Klaas, D. M.; Viswanath, D. S. *Ind. Eng. Chem. Res.* 1998, 37, 2064–2068.

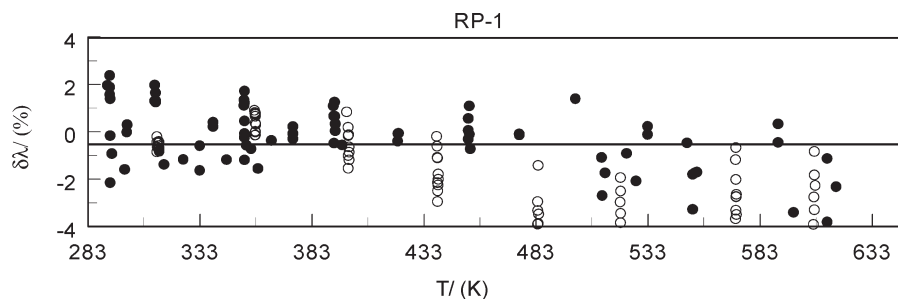


Figure 3. Percentage thermal conductivity deviations, $\delta\lambda = 100(1 - \lambda_{\text{cal}}/\lambda_{\text{exp}})$, of the present and reported¹ experimental thermal conductivities from the values calculated with surrogate model.¹ (●), this work; (○), Magee et al.¹

determined the values of the empirical parameter n for various homologous series (n -alkanes, alcohols, halogen, paraffin hydrocarbons, aromatic hydrocarbons, etc.) with experimental thermal conductivity data. The derived values of n varied from 0.6 (for alcohols) to 0.943 (for paraffins). We used the relation 3 to compare with the present data for the RP-1, sample A. The present thermal conductivity data for RP-1 (sample A) were fitted to eq 3. The derived value of parameter n is 0.55. Calculated values are presented in Figure 1 for some selected isobars with $n = 0.55$ and $T_0 = 293$ K. As one can see, the agreement is good over the whole measured temperature range and at pressures up to 60 MPa (AAD within 0.4–2.5% depending on pressure). Equation 3 can be used to accurately predict (within 2.0%) the thermal conductivity of RP-1 just by knowing the thermal conductivity of RP-1 at reference temperature $T_0 = 293$ K, $\lambda_0(P, T_0)$ for each isobar.

Conclusions

New thermal conductivity data for rocket propellant (RP-1 fuel) have been measured with a coaxial-cylinder (steady-state) technique in the temperature range from 292 to 732 K and at pressures up to 60 MPa. Although the composition of this sample was unusual, the results are important in that they illustrate the importance of compositional variability of complex fluids on transport property measurements. The temperature and pressure dependences of thermal conductivity

were studied. A significant effect (within 5–10% and more) of thermal decomposition (thermal stress) on the measured values of the thermal conductivity of RP-1 (sample A) at high temperatures (around 650 K) was found. The measured values of thermal conductivity of RP-1 agreed well (within 1.0%) with the reported data and the values calculated with a reference correlation equation for a surrogate hydrocarbon mixture. An empirical prediction equation for thermal conductivity of RP-1 was developed by use of the present experimental data (sample A). The model provides a reliable calculation of the thermal conductivity of this fluid with the input of minimal experimental information; namely, the thermal conductivity of RP-1 as a function of pressure at reference temperature $T_0 = 293$ K, $\lambda_0(P)$. The AAD between measured and predicted values of thermal conductivity for this sample of RP-1 is 0.4–2.5%.

Acknowledgment. I. M. A. thanks the Thermophysical Properties Division at the National Institute of Standards and Technology for the opportunity to work as a Guest Researcher at NIST during the course of this research. The authors would like to thank Dr. N. Azizov for his assistance in preparing the experimental apparatus to measure the thermal conductivity. The authors also thank Dr. Magee and Dr. Huber of NIST for helpful discussions, for providing the samples of RP-1, and for providing the surrogate model for RP-1. Part of this work was financially supported by the NIST.